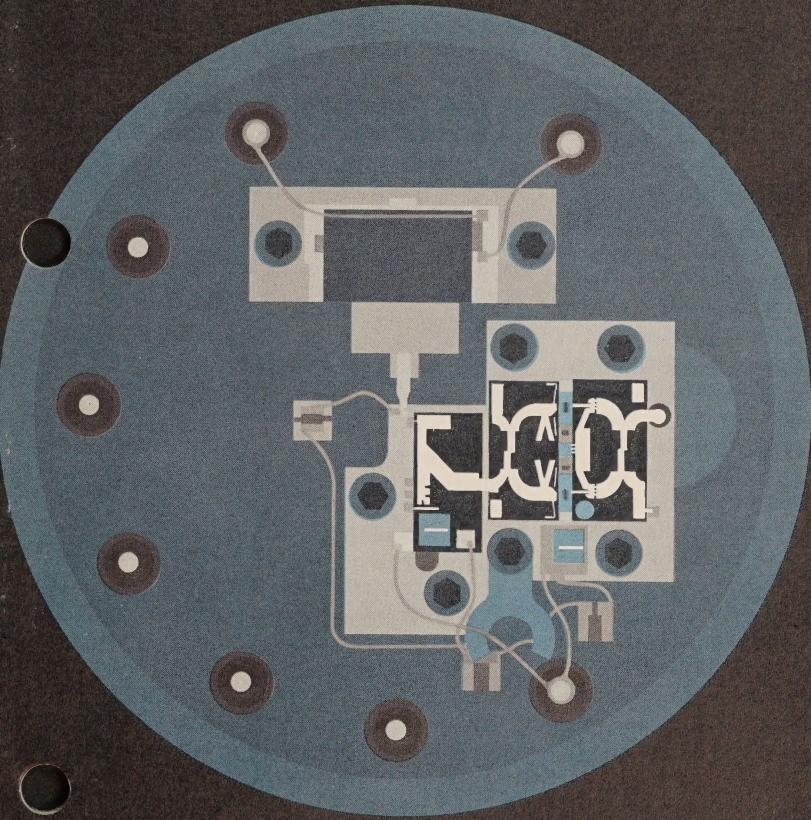


# YIG-Tuned FET Oscillator Design 8-18 GHz



WATKINS-JOHNSON COMPANY

# Tech-notes

Recent developments at Watkins-Johnson Company have led to the introduction of an 8- to 18-GHz YIG-tuned FET oscillator. Compared with the Gunn oscillator, the YIG-tuned FET oscillator provides significantly more power output, improved efficiency, and greater reliability.

This article deals with the design and construction of a YIG-tuned FET oscillator that is tunable over the entire 8- to 18-GHz range. The minimum output power from the oscillator operating into a 50-ohm load is about +6 dBm. The addition of a balanced buffer amplifier increases the power to about +12 dBm minimum. When optimized for the 12- to 18-GHz band, the oscillator alone generates a minimum of +10 dBm. The oscillator/amplifier combination produces at least +15 dBm. This article presents a design technique of general applicability to transistor oscillator design and discusses a number of difficulties inherent in the design of broadband oscillators, especially fixed-frequency resonances, linearity, and power dropouts at the low end of the frequency range.

Broadband tunable oscillators operating at frequencies above 8 GHz have traditionally used bulk-effect diodes as the active elements. With the introduction of 1-micron and 0.5-micron gate-length field-effect transistors (FET's), serious competition has developed for the diode oscillators. The improved efficiency and reliability of FET's compared with Gunn-effect devices makes them especially attractive for application where low dc power consumption is important, such as in aircraft applications.

With only a few exceptions, literature<sup>1-4</sup> on FET oscillators has concentrated on narrow-band devices with bandwidths of less than 10%<sup>5-9</sup>. Also, most work to date has been performed at frequencies below 12 GHz, although recently some results have been reported in the 8- to 18-GHz range<sup>13</sup>. However, the circuits developed in this

recent work produce substantially less power than the circuit described in this article.

The techniques presented here are employed in the design of a fundamental oscillator that is tunable by means of a YIG resonator over the entire 8- to 18-GHz frequency range. The construction details of the oscillator are described and data on a typical unit are presented.

## Oscillator Design

Table 1 shows the common-source S-parameters of the device initially chosen for this design, the NEC-388 FET manufactured by Nippon Electric Corporation. Since the measurements are made using a test fixture that closely resembles the final circuit, parasitic bonding inductances are already included in the S-parameters and need not be taken into account at a later stage in the design.

A typical oscillator topology is shown in Figure 1. It consists of a YIG resonator described by the complex reflection coefficient  $\Gamma_R$ , a load characterized by the reflection coefficient  $\Gamma_L$ , and a circuit containing the active device which when connected to the load is characterized by the reflection coefficient  $S_{11}$ . The conditions necessary for oscillation to start are  $\Gamma_R S_{11} = 1$  or  $\Gamma_L S_{22} = 1$ . The two conditions are equivalent<sup>10</sup>, so only the first is employed:

$$|\Gamma_R||S'_{11}| e^{i(\theta_R + \theta S'_{11})} = 1 \quad (1)$$

or

$$|\Gamma_R||S'_{11}| = 1 \quad (2)$$

and

$$\theta_R + \theta S'_{11} = 0 \quad (3)$$

Equation (2) is the condition for steady-state oscillation. Once oscillations begin,  $S'_{11}$  changes from the

Table 1. Watkins-Johnson FET amplifier measurement.

FREQ (MHz)	S <sub>11</sub>		S <sub>21</sub>		S <sub>12</sub>		S <sub>22</sub>	
	MAG	ANG	MAG	ANG	MAG	ANG	MAG	ANG
8000.00	0.760	-91	1.757	98	0.075	41	0.665	-39
9000.00	0.758	-104	1.661	89	0.073	40	0.642	-49
10000.00	0.755	-118	1.571	80	0.071	39	0.655	-57
11000.00	0.756	-113	1.473	72	0.067	35	0.710	-64
12000.00	0.701	-122	1.388	66	0.060	50	0.716	-64
13000.00	0.677	-135	1.288	56	0.061	45	0.674	-71
14000.00	0.670	-145	1.154	48	0.063	51	0.646	-81
15000.00	0.685	-149	1.067	44	0.057	57	0.670	-88
16000.00	0.723	-155	1.021	40	0.112	59	0.660	-95
17000.00	0.709	-160	1.049	35	0.105	29	0.657	-94
18000.00	0.720	-161	0.955	27	0.086	22	0.714	-96

small-signal values used here. Therefore, the condition for oscillation to start is taken to be,

$$|\Gamma_R||S'_{11}| \geq 1 \quad (4)$$

where  $S'_{11}$  is the small-signal value. Oscillations will build from the small-signal conditions, and  $S'_{11}$  changes until it satisfies Equation (2).

It will be shown later that, for a YIG resonator operating in the frequency band of interest,  $|\Gamma_R| \approx 1$ . Therefore, the following can be taken as the condition for oscillation:

$$|S'_{11}| \geq 1 \quad (5)$$

## The Feedback Scheme

The FET can be imbedded in a variety of circuits which produce sufficient feedback to satisfy Equation (5). There are three possible series feedback circuits and three parallel feedback circuits shown in Figure 2. The block labeled "X" represents a reactive circuit.

The circuit for this design is the common-gate series circuit with an inductor serving as the feedback element. Since the parallel-feedback type circuits require dc blocks in the feedback loop, they are more susceptible to problems due to the severe

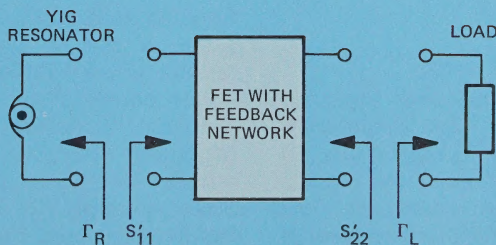


Figure 1. Typical oscillator circuit topology with YIG resonator, active element, and matching network.

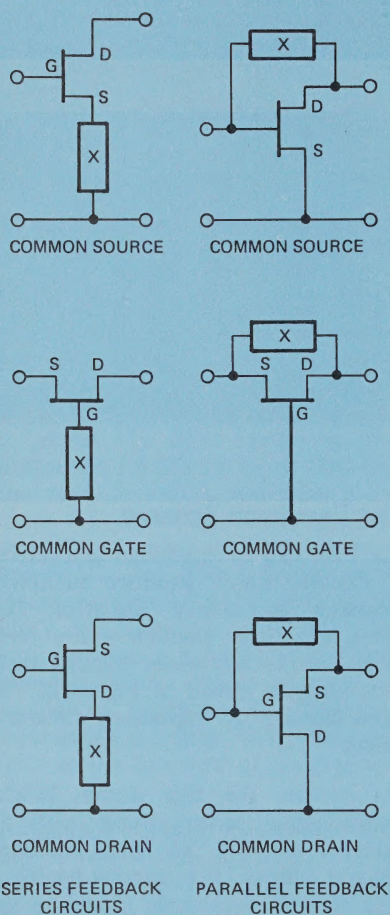


Figure 2. Possible feedback schemes showing series and parallel-type networks.

parasitics of the blocking capacitor that may occur at high frequencies. Inductive feedback is preferable to capacitive feedback when the circuits are constructed in microstrip. The inductance of the feedback element is easy to adjust for optimum performance, while the capacitance is difficult to change. Finally, the common-gate configuration has the advantage over common-source and common-

drain because the gate is operated dc grounded. This eliminates the need for any dc blocks or rf shorts in the feedback circuit, thereby further eliminating parasitics. The complete circuit is shown in Figure 3.

The first step in the design is the calculation of the common-gate S-parameters of the FET for various values of feedback inductance. Table 2 lists the S-parameters for 0.3, 0.5, and 1.0 nH inductance. Note that for 1 nH,  $|S_{11}|$  is greater than 1 from about 9 GHz to 13 GHz, so oscillations will occur over this frequency range without a matching network; a 50-ohm load is all that is required. As the inductance decreases,  $|S_{11}|$  peaks at higher frequencies. However, for the transistor under consideration (NEC 388), there is no value of inductance that makes  $|S_{11}| > 1$  above 14 GHz. To obtain oscillation above 14 GHz, a matching network must be placed between the drain and the 50-ohm load.

If the matching network is characterized by a reflection coefficient  $\Gamma_L$  (see Figure 3), then

$$S'_{11} = S_{11} + \frac{S_{12} S_{21}}{\frac{1}{\Gamma_L} - S_{22}} \quad (6)$$

The objective is to choose a  $\Gamma_L$  at all frequencies of interest so that  $|S'_{11}| > 1$  for a particular feedback inductance.

Looking at a Smith chart for the  $S'_{11}$  plane, it can be seen that the condition  $|S'_{11}| = 1$  defines a circle which is the border of the chart. It divides the plane into two regions, one inside the circle having  $|S'_{11}| < 1$  and one outside the circle with  $|S'_{11}| > 1$ . Since equation (6) is bilinear in the variables  $S'_{11}$  and  $\Gamma_L$ , it follows that circles in the  $S'_{11}$  plane are mapped into circles in the  $\Gamma_L$  plane. The circle in the  $\Gamma_L$  plane, like the corresponding one in the  $S'_{11}$  plane, will divide the  $\Gamma_L$  plane into two regions,

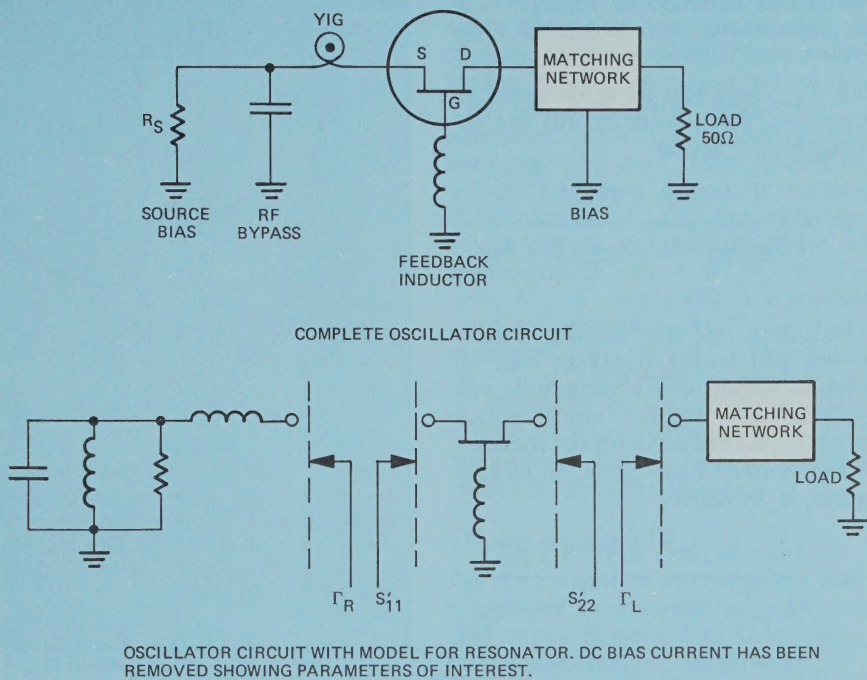


Figure 3. Complete oscillator circuit including parallel resonant circuit model for YIG.

Table 2. Common Gate S-Parameters.

FREQ (MHz)	$S_{11}$		$S_{12}$		$S_{21}$		$S_{22}$	
	MAG	ANG	MAG	ANG	MAG	ANG	MAG	ANG
0.3 nH FEEDBACK								
8000	0.319	177.7	0.149	49.39	1.313	-41.4	1.045	-25.7
10000	0.487	172.9	0.161	58.70	1.526	-61.5	1.269	-40.8
12000	0.586	159.2	0.194	79.80	1.798	-88.7	1.584	-55.4
14000	0.801	113.0	0.539	88.30	1.910	201.0	1.670	251.0
16000	0.754	88.7	0.755	74.35	1.630	150.0	1.430	212.0
18000	0.495	65.1	0.824	57.40	1.465	113.0	0.949	189.3
0.5 nH FEEDBACK								
8000	0.438	170.0	0.124	66.8	1.450	-45.4	1.103	-27.1
10000	0.792	157.0	0.185	114.0	1.950	-74.0	1.490	-46.6
12000	1.219	124.3	0.536	121.6	2.830	239.0	2.100	-75.2
14000	0.919	53.8	0.943	62.7	1.850	140.0	1.151	209.0
16000	0.611	36.7	0.934	47.5	1.320	98.5	0.698	179.9
18000	0.433	181.0	0.191	48.6	1.210	77.7	0.383	169.0
1.0 nH FEEDBACK								
8000	0.954	153.7	0.216	134.0	2.038	-59.4	1.335	-33.5
10000	2.690	84.47	1.378	103.2	4.154	210.0	2.300	257.1
12000	1.431	14.69	1.150	50.2	2.184	122.0	0.8114	200.0
14000	0.645	-0.248	0.897	34.7	1.099	78.2	0.1720	191.0
16000	0.450	-5.430	0.883	29.6	0.976	56.2	0.0757	176.8
18000	0.386	-17.4	0.861	29.2	0.976	48.9	0.0528	-67.4

that which corresponds to  $|S'_{11}| < 1$  and that which corresponds to  $|S'_{11}| > 1$ .

This  $\Gamma_L$  circle can be constructed in two ways. First, equation (6) can be solved for  $\Gamma_L$ , giving

$$\Gamma_L = \frac{S'_{11} - S_{11}}{S_{12} S_{21} + S'_{11} S_{22} - S_{11} S_{22}} \quad (7)$$

Substituting in the known S-parameters and letting  $S'_{11}$  vary over all complex values of unit magnitude will produce the required circle. Alternatively, one can solve for the location of the center of the circle, M, and its radius, R, by solving<sup>11</sup>

$$M = \frac{S_{22}^* - S_{11}(S_{11}^* S_{22}^* - S_{12}^* S_{21}^*)}{|S_{22}|^2 - |S_{11} S_{22} - S_{12} S_{21}|^2} \quad (8)$$

$$R = \frac{|S_{12} S_{21}|}{|S_{22}|^2 - |S_{11} S_{22} - S_{12} S_{21}|^2} \quad (9)$$

where,  $S_{ij}^*$  = complex conjugate of  $S_{ij}$ . Once the circle is plotted, the remaining task is to determine whether the region inside or outside the circle is the unstable ( $|S'_{11}| > 1$ ) one. This can be done immediately by noting that the center of the chart,  $\Gamma_L = 0$ , corresponds to  $S'_{11} = S_{11}$ . Since  $S_{11}$  is known from Table 2, it is apparent whether the center of the chart is stable ( $|S'_{11}| < 1$ ) or unstable ( $|S'_{11}| > 1$ ). Since the circle divides the chart into two regions, the region which includes the center has the same stability as the center, while the other region has the opposite stability. Figure 4 shows these circles plotted for 1 nH feedback inductance, with arrows pointing toward the unstable region.

Also plotted in Figure 4 is a trajectory of  $\Gamma_L$  with frequency that would be sufficient to produce oscil-

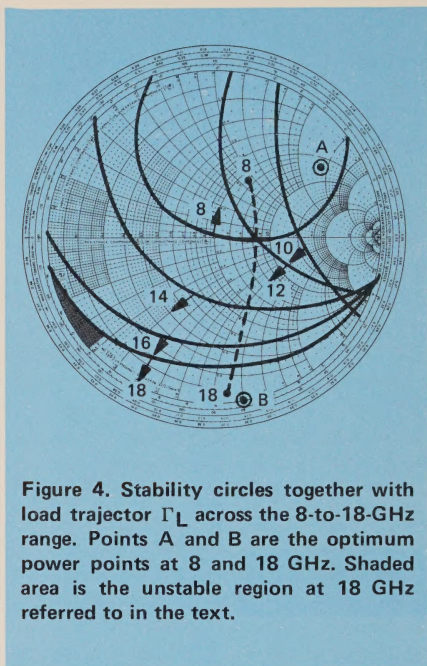


Figure 4. Stability circles together with load trajectory  $\Gamma_L$  across the 8-to-18-GHz range. Points A and B are the optimum power points at 8 and 18 GHz. Shaded area is the unstable region at 18 GHz referred to in the text.

lations across the 8-18 GHz range. The design problem then becomes the construction of a matching circuit that is described by a  $\Gamma_L$ , similar to that in the figure.

Two questions are relevant to the construction of the matching circuit: 1) among all the possible loads similar to that in Figure 4, what is the "ideal" load (that which produces maximum power output)? 2) are there some loads that produce spurious oscillations?

Although the question of maximum power is complicated by the fact that the maximum power state may be a large-signal state, it can be expected that the optimum load points be near the maximum of  $|S'_{11}|$ . As  $\Gamma_L$  is made to vary,  $|S'_{11}|$  will vary according to Equation (6). Clearly, if  $|S_{22}| > 1$ , then there is some value of  $|\Gamma_L| < 1$  such that

$$\frac{1}{\Gamma_L} = S_{22}.$$

At this point, Equation (6) becomes infinite, producing a maximum of  $S'_{11}$ . If, instead,  $|S_{22}| < 1$ , then the point

$$\frac{1}{\Gamma_L} = S_{22},$$

is outside the chart and  $S'_{11}$  is an analytic function of  $\Gamma_L$ . The maximum-modulus theorem<sup>12</sup> then tells us that the maximum of  $|S'_{11}|$  occurs on the boundary of the chart. As an example of the first case, at 8 GHz, according to Table 2, the maximum occurs at

$$\Gamma_L = \frac{1}{1.335} e^{j33.5^\circ}$$

which is plotted as point A in Figure 4. At 18 GHz the maximum occurs at the boundary. Figure 5 shows  $|S'_{11}|$  plotted as a function of the angle of  $\Gamma_L$  for  $|\Gamma_L| = 0.9$ , and  $|\Gamma_L| = 1.0$ . There is a gentle maximum around  $275^\circ$ , indicating that the power is not a strong function of the match at the higher frequencies. This point is plotted in Figure 4 as point B.

At the higher frequencies, the important restriction on the match is spurious oscillations rather than power. If the impedance presented to the YIG is sufficiently capacitive, a resonance with the inductive YIG coupling loop may occur, producing a fixed frequency output. If the loop inductance is 1 nH, the reflection coefficient of the resonator will be approximately  $\Gamma_R = e^{j145^\circ}$ . So, for  $\angle S_{11} \leq -45^\circ$ , there will be a possible spurious oscillation. At  $|\Gamma_L| = 1$  the condition  $\angle S'_{11} \leq -45^\circ$  corresponds to  $\angle \Gamma_L \leq -139^\circ$ ; so the shaded area in Figure 4 is potentially unstable against spurious oscillation and should be avoided. Larger loop inductances make the spurious area larger.

### Effects of the YIG

The YIG together with coupling loop is modeled in Figure 3 as a parallel RLC circuit in series with an inductor. The element values<sup>13</sup> are given by

$$L = \frac{R}{Q\omega_0} \quad (10)$$

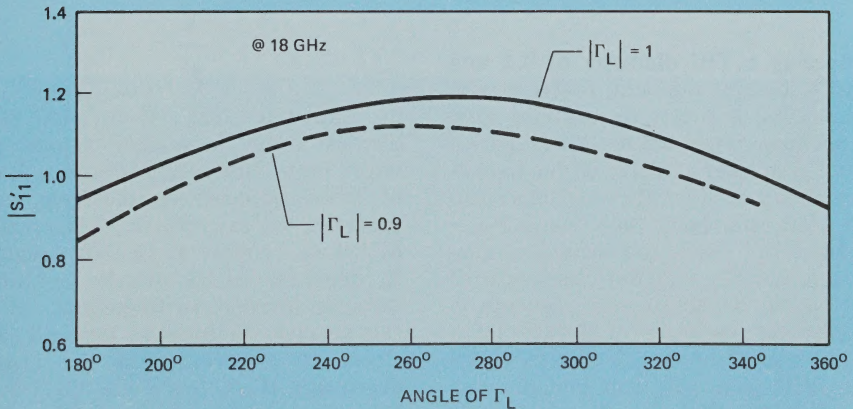


Figure 5. The maximum value of  $|S'_{11}|$  occurs on the boundary of the Smith Chart at an angle of  $270^\circ$ .

$$C = \frac{1}{L\omega_o^2} = \frac{Q}{R\omega_o} \quad (11)$$

$$R = \mu_o \frac{V}{d^2} Q(2\pi\gamma)(4\pi M_s) \quad (12)$$

where  $\omega_o$  is the frequency to which the YIG is tuned,  $V$  is the sphere volume,  $d$  is the diameter of the coupling loop,  $Q$  is the unloaded  $Q$  of the sphere,  $\mu_o$  is the permeability of free space ( $4\pi \times 10^{-7}$  newtons/(ampere)<sup>2</sup>),  $\gamma$  is the gyromagnetic ratio of the electron (2.8 MHz/gauss), and  $4\pi M_s$  is the saturation magnetization (1750 gauss in the case of pure YIG).

The impedance of the resonator becomes:

$$Z_R(\omega) = \frac{R}{1 + Q^2 \left( \frac{\omega}{\omega_o} - \frac{\omega_o}{\omega} \right)^2} + j \omega L_{\text{Loop}} + \frac{RQ \left( \frac{\omega_o}{\omega} - \frac{\omega}{\omega_o} \right)}{1 + Q^2 \left( \frac{\omega}{\omega_o} - \frac{\omega_o}{\omega} \right)^2} \quad (13)$$

Choosing a YIG diameter of 0.2 mm and a loop of 0.5 mm, together with  $Q = 2000$  and 0.1 nH coupling loop inductance, gives the result in Figure 6 for  $\Gamma_R$  at near 12 GHz. If the matching circuit at 12 GHz were chosen to be a 50 ohm load, then  $S'_{11} = S_{11} = 1.43 e^{j14.7^\circ}$ . Since the oscillation condition is  $\angle \Gamma_R = -\angle S'_{11}$ , the angle of  $\Gamma_R$  must be about  $-14^\circ$ , giving an oscillation frequency of about 12.016 GHz, instead of the 12 GHz to which the YIG is tuned. This phenomenon is called "pulling," and causes oscillator non-linearity with tuning current. To improve the linearity, it is necessary to spread the plot in Figure 6 so that, for example, the 12.02 GHz

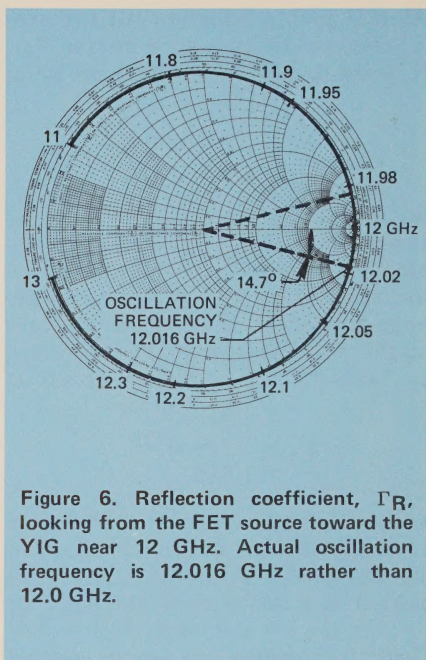


Figure 6. Reflection coefficient,  $\Gamma_R$ , looking from the FET source toward the YIG near 12 GHz. Actual oscillation frequency is 12.016 GHz rather than 12.0 GHz.

point is moved to the location of the 12.05 GHz point. This brings the oscillation frequency at  $-14^\circ$  closer to  $\omega_o$ . This spreading can be accomplished by decreasing  $R$ , which, in turn, can be done by decreasing

$$\frac{V}{d^2}$$

in Equation (12). Physically, this implies using a smaller sphere or larger loop. However, there is a limit to this procedure. As the frequency decreases to, say, 8 GHz,  $R$  decreases to 2/3 of its value at 12 GHz because  $R$  depends on  $Q$ , which, in turn, depends linearly on frequency. As  $R$  gets smaller, the locus in Figure 6 gets closer to the center of the chart, decreasing  $|\Gamma_R|$ . Since  $|\Gamma_R||S_{11}| = 1$  is necessary for oscillation, the oscillation will cease if  $|\Gamma_R|$  decreases too much. Thus, the price of good linearity is the possibility of power dropouts at the low end of the frequency band.

## Design of the Circuit

Designing a circuit that produces a  $\Gamma_L$  like that shown in Figure 4 is basically a trial-and-error procedure — no direct synthesis technique exists. The network chosen is a microstrip filter structure as shown in Figure 7. The shorted stub provides the means for biasing the drain of the FET. The match provided by this circuit is shown in Figure 8, plotted atop the stability circles that result from 0.6 nH feedback inductance.

## Circuit Construction

The circuit was fabricated on a 0.38-mm thick, fused-silica substrate, using thin-film MIC technology.

The unpackaged GaAs FET chip was die-attached directly to a gold-plated molybdenum carrier whose thermal coefficient of expansion approximates that of fused silica. Molybdenum was used also because it is non-magnetic.

To minimize the stray circuit parasitics, the FET was die-attached as close as possible to the circuit with minimum lead lengths. Source inductance was minimized by using a 0.025 mm  $\times$  0.635 mm gold ribbon for the YIG coupling loop and an Au wire mesh

was used to bond from the source pad of the FET to the coupling loop. A 3-terminal chip voltage regulator was die-attached to the circuit to provide a regulated bias voltage to the FET and also used to suppress any transients which could damage the FET.

An electronically regulated heater circuit was incorporated which provided temperature variations of less than  $\pm 1^\circ\text{C}$  to the YIG sphere from  $-54^\circ\text{C}$  to  $+85^\circ\text{C}$ .

The entire circuit was enclosed in a magnetic shell housing which was hermetically sealed by welding.

Figure 9 is a photograph of the oscillator circuit followed by a buffer amplifier. The buffer amplifier improves the output power by about 5 dB and provides 15 to 20 dB of isolation from load variations.

The transistor used in the construction had S-parameters similar to those used in the design stages, with saturated drain-source current of  $I_{DSS} = 60$  mA and transconductance of  $g_m = 40$  mmho.

## Experimental Results

Output power versus frequency is shown in Figure 10. The power with-

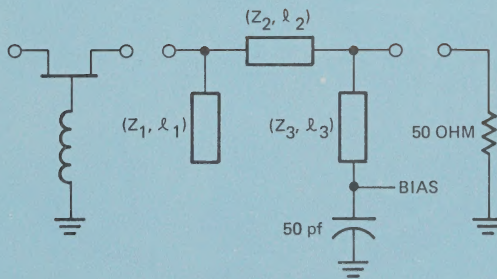
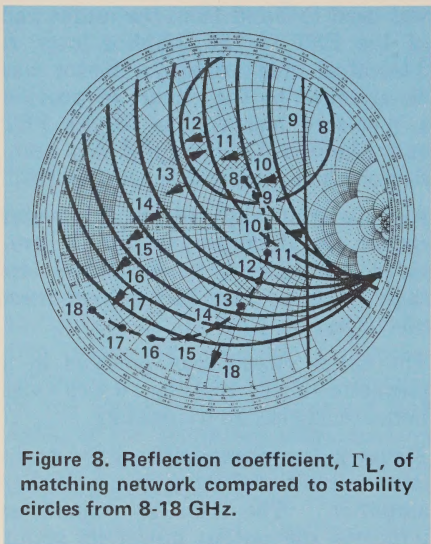


Figure 7. Network chosen to provide 8-18 GHz match.



out the amplifier varies from +6 dBm minimum to +16 dBm maximum. The addition of the buffer amplifier improves the output power by about 5 dB.

With the gate inductance decreased and the circuit optimized for the 12-18 GHz band, minimum power improved to 10.8 dBm for the oscillator alone. Data are displayed in Figure 11. The transistor operating conditions for all this data were about 50 mA ( $I_{DS}$ ) and 5 volts ( $V_{DS}$ ), giving a peak efficiency of 16%.

### Conclusions

This article presents results on a YIG-tuned FET oscillator that is tunable over the entire 8- to 18-GHz band. The

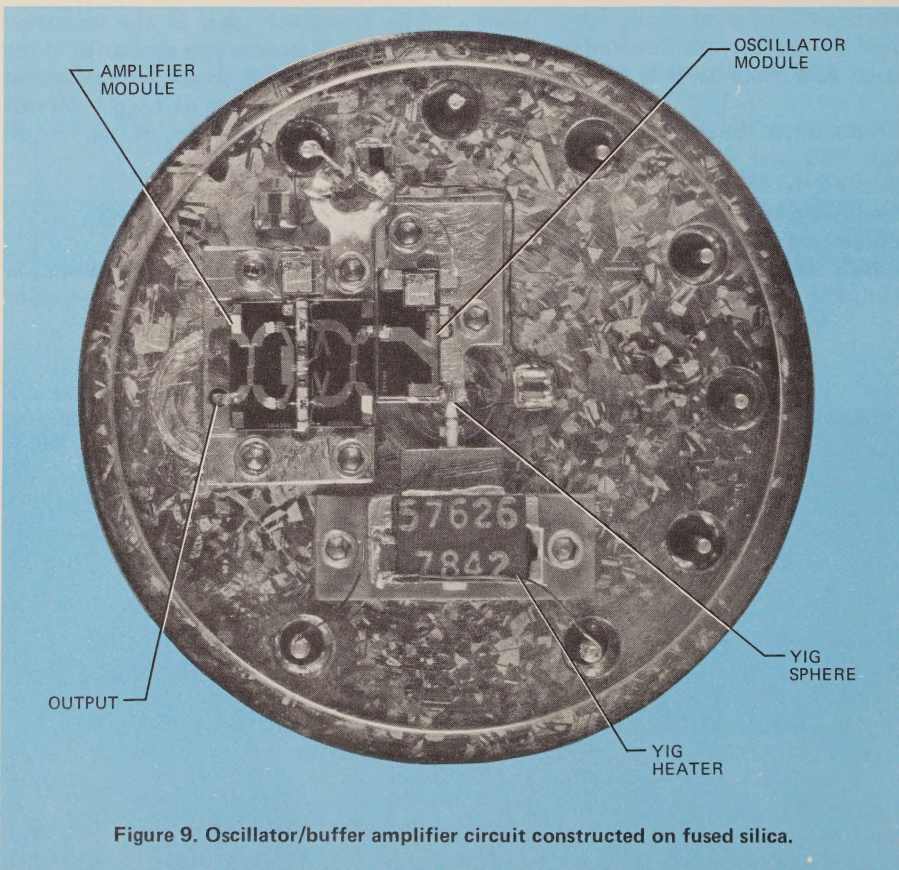


Figure 9. Oscillator/buffer amplifier circuit constructed on fused silica.

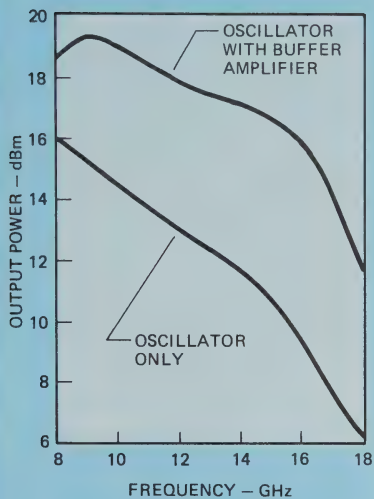


Figure 10. Power output versus frequency across the 8- to 18-GHz band for the oscillator with and without buffer amplifier.

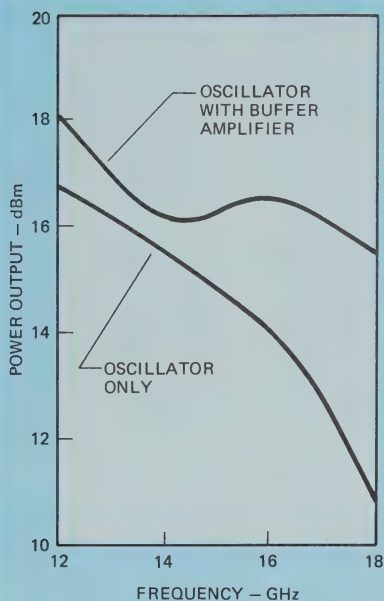


Figure 11. Power output with the circuit optimized for the 12- to 18-GHz band.

oscillator, coupled with a buffer amplifier, produces 11.8 dBm of power. A general design technique is used which is applicable to wideband transistor oscillators at all frequencies.

Also pointed out in detail are the effects of the resonator circuit on linearity and low-frequency dropouts, and the means of avoiding spurious oscillations.



## References

1. Trew, Robert J. "Design Theory for Broad-band YIG-tuned FET Oscillators," *IEEE Transactions, Microwave Theory Techniques*, Vol. MTTT-27, (January 1979), pp. 8-14.
2. Heyboer, T. L. and F. E. Emery. "YIG-tuned GaAs FET Oscillators," *IEEE MTT-S International Microwave Symposium Digest*, (1976), pp. 48-50.

3. Ruttan, T. "X-Band GaAs FET YIG-tuned Oscillators," *IEEE MTTT-S International Microwave Symposium Digest*, (1977), pp. 264-266.
4. Tserng, H. Q. and H. M. Macksey. "Wide-band Varactor-tuned GaAs MESFET Oscillators at X- and Ku-bands," *IEEE MTTT-S International Microwave Symposium Digest*, (1977), pp. 267-269.
5. Maed, M.; S. Takahashi; and H. Kodera. "CW Oscillation Characteristics of GaAs Schottky-barrier Gate, Field-effect Transistors," *Proceedings of the IEEE*, Vol. 63, (February 1975), pp. 320-321.
6. Pucel, R. A.; R. Bera; and D. Masse. "Experiments on Integrated Gallium-arsenide FET Oscillators at X-band," *Electronics Letters*, Vol. 11, (May 1975), pp. 219-220.
7. Slaymaker, N. A. and J. A. Turner. "Alumina Microstrip GaAs FET 11 GHz Oscillator," *Electronics Letters*, Vol. 11, (May 1975), pp. 300-301.
8. Omori, M. and C. Nishimoto. "Common-gate GaAs FET Oscillator," *Electronics Letters*, Vol. 11, (August 1975), pp. 369-371.
9. Maeda, M.; K. Kimura; and H. Kodera. "Design and Performance of X-band Oscillators with GaAs Schottky-gate, Field-effect Transistors," *IEEE Transactions, Microwave Theory Techniques*, Vol. MTT-23, (August 1975), pp. 661-667.
10. Basawapatna, Ganesh R. and Roger Stancliff. "A Unified Approach to the Design of Wide-band Microwave Solid-state Oscillators," Unpublished.
11. Carson, Ralph S. *High Frequency Amplifiers*. New York: John Wiley and Sons, Inc., 1975, p. 193.
12. Churchill, Ruel V. *Complex Variables and Applications*, New York: McGraw Hill Book Co., Inc., 1960, p. 124.
13. Oyafuso, Robert T. "An 8-18 GHz FET YIG-tuned Oscillator," *IEEE MTTT-S International Microwave Symposium Digest*, (1979), pp. 183-184.

## Acknowledgements

The authors wish to thank Mr. Robert Suzuki for his work in aligning and tuning the oscillator, and Dr. Karl

Nielas for help with a number of the calculations.

## Authors:



### Dr. James C. Papp

As Head of the Watkins-Johnson Company Converter Section, Dr. Papp is responsible for design, development, and production of microwave converters and microwave mixers that operate at 2-to-18 GHz. Recently, the Converter Section has been responsible for the design and production of converters for the B-52 Power Management System, the Aegis Shipboard Weapon System, the F-15 ECM Suite, the F-18 Radar System, and for a variety of commercial applications, such as satellite ground terminals.

Previously, Dr. Papp was Head of the Watkins-Johnson YIG engineering

Section, where he was responsible for product development of YIG devices, including band-pass filters, band reject filters, harmonic generators, and transistor and bulk-effect oscillators. He was also responsible for engineering support for YIG devices built in the production section.

Dr. Papp received an A.B., Physics, with distinction, and Ph.D, Physics, from the University of California, Berkeley. He is a member of the American Physical Society, IEEE, and Phi Beta Kappa.



## Yoshiomi Y. Koyano

Mr. Koyano is a Member of the Technical Staff, Watkins-Johnson Company, Solid State Division. He is currently involved in the design and development of thin-film, YIG-tuned field-effect transistor oscillators and buffer amplifiers. Mr. Koyano is in charge of the effort to develop the X-band, Ku band, and the 8-18 GHz oscillators. He was in charge of the development effort on the 2-6 GHz and 2-8 GHz bipolar transistor oscillator as well as the high power 4-8 GHz oscillator. Prior to his work on thin-film circuits, Mr. Koyano was

responsible for the design of integrated filter/oscillators in the C, X, and Ku bands, and for the production engineering of YIG-tuned GaAs oscillators and transistor oscillators. In addition, he was project engineer for the design and development of high-power L-band transistor oscillators for missile applications.

Mr. Koyano attended Milwaukee School of Engineering and the U.S. Army Microwave School at Ft. Monmouth, New Jersey.





WATKINS-JOHNSON

**Manufacturing  
and Office Locations**

**United States**

**SALES OFFICES**

**CALIFORNIA**

Watkins-Johnson  
3333 Hillview Avenue  
Palo Alto 94304  
Telephone: (415) 493-4141

Watkins-Johnson  
2525 North First Street  
San Jose, 95131  
Telephone: (408) 262-1411

Watkins-Johnson  
831 South Douglas Street  
Suite 131  
El Segundo 90245  
Telephone: (213) 640-1980

**DISTRICT OF COLUMBIA**

Watkins-Johnson  
700 Quince Orchard Road  
Gaithersburg, Md. 20760  
Telephone: (301) 948-7550

**FLORIDA**

Watkins-Johnson  
325 Whooping Loop  
Altamonte Springs 32701  
Telephone: (305) 834-8840

**MARYLAND**

Watkins-Johnson  
700 Quince Orchard Road  
Gaithersburg 20760  
Telephone: (301) 948-7550

**MASSACHUSETTS**

Watkins-Johnson  
5 Militia Drive  
Suite 11  
Lexington 02173  
Telephone: (617) 861-1580

**PENNSYLVANIA**

Watkins-Johnson  
385 Lancaster Avenue  
Haverford 19041  
Telephone: (215) 896-5854

**OHIO**

Watkins-Johnson  
2500 National Road  
Suite 200  
Fairborn 45324  
Telephone: (513) 426-8303

**TEXAS**

Watkins-Johnson  
9216 Markville Drive  
Dallas 75243  
Telephone: (214) 234-5396

**International**

**ITALY**

Watkins-Johnson Italiana  
S.p.A.  
Piazza G. Marconi, 25  
00144 Roma-EUR  
Telephone: 59 45 54  
Telex: 63278  
Cable: WJROM-ROMA

**GERMANY, FEDERAL  
REPUBLIC OF**

Watkins-Johnson  
Manzingerweg 7  
8009 Muenchen 60  
Telephone: (089) 836011  
Telex: 529401  
Cable: WJDBM-MUENCHEN

**UNITED KINGDOM**

Watkins-Johnson  
Shirley Avenue  
Windsor, Berkshire SL4 5JU  
Telephone: Windsor 69241  
Telex: 847578  
Cable: WJUKW-WINDSOR

The Watkins-Johnson Tech-notes is a bi-monthly periodical circulated to educational institutions, engineers, managers of companies or government agencies, and technicians. Individuals may receive issues of Tech-notes by sending their subscription request on company letterhead, stating position and nature of business to the Editor, Tech-notes, Palo Alto, California. Permission to reprint articles may also be obtained by writing the Editor.